

## Multiple Grains in Nanocrystals: Effect of Initial Shape and Size on Transformed Structures Under Pressure

Sanjay Kodiyalam,<sup>1</sup> Rajiv K. Kalia,<sup>2</sup> Aiichiro Nakano,<sup>2</sup> and Priya Vashishta<sup>2</sup>

<sup>1</sup>*Biological Computation and Visualization Center, Department of Physics & Astronomy and Department of Computer Science, Louisiana State University, Baton Rouge, LA 70803-4001, USA*

<sup>2</sup>*Collaboratory for Advanced Computing and Simulations, Departments of Material Science & Engineering, Physics & Astronomy, Computer Science, and Biomedical Engineering, University of Southern California, Los Angeles, CA 90089-0242, USA*  
(Received 3 June 2004; published 11 November 2004)

Pressure-induced structural transformations in spherical and faceted gallium arsenide nanocrystals of various shapes and sizes are investigated with a parallel molecular-dynamics approach. The results show that the pressure for zinc blende to rocksalt structural transformation depends on the nanocrystal size, and all nanocrystals undergo nonuniform deformation during the transformation. Spherical nanocrystals above a critical diameter  $\geq 44$  Å transform with grain boundaries. Faceted nanocrystals of comparable size have grain boundaries in 60% of the cases, whereas the other 40% are free of grain boundaries. The structure of transformed nanocrystals shows that domain orientation and strain relative to the initial zinc blende lattice are not equivalent. These observations may have implications in interpreting the experimental x-ray line shapes from transformed nanocrystals.

DOI: 10.1103/PhysRevLett.93.203401

PACS numbers: 36.40.Ei, 61.50.Ks, 61.72.Mm, 81.30.Hd

A confluence of ideas and expertise from different disciplines is giving birth to numerous exciting applications of nanocrystals in optoelectronics, hybrid inorganic-biomolecular systems, and novel nanostructured materials. These applications exploit the sensitive physical and chemical characteristics of nanocrystals, which arise from the preponderance of surface atoms [1,2]. Surface effects play a vital role in the size dependence of solid-solid structural transformations. In semiconductor nanocrystals, the observed *increase* in pressure for solid-solid structural transformation relative to the bulk [3] is due to surface effects. During the transformation, nanocrystals change shapes coherently by undergoing uniform deformation [3]. The observed *decrease* in the transition pressure for structural transformation of iron oxide nanocrystals [4] has been attributed to an increase in the bulk modulus of these nanocrystals. This explanation holds for lead sulphide nanocrystals where an increase in the transition pressure and a decrease in bulk modulus have been observed [5]. In this Letter, we report on molecular-dynamics (MD) simulations of Ga-As nanocrystals, where we observe considerable size and shape dependence of pressure-induced structural transformation from the fourfold coordinated zinc blende structure to the sixfold coordinated rocksalt structure. In spherical nanoparticles of diameter  $\geq 4.4$  nm, nanoscale grain boundaries with different domain orientations are found during and after the transformation. In contrast, forty percent of the faceted nanocrystals of comparable size undergo the transformation without any grain boundaries. These results have important implications on the interpretation of x-ray data for structural transformations in Ga-As nanocrystals.

Molecular-dynamics simulations on Ga-As nanocrystals are based on an interatomic potential that consists of a combination of two-body and three-body interactions [6]:

$$V_{ij}^2 = \frac{H_{ij}}{r_{ij}^{\eta_{ij}}} + \frac{Z_i Z_j}{r_{ij}} e^{(-r_{ij}/r_{1s})} + \frac{D_{ij}}{r_{ij}^4} e^{(-r_{ij}/r_{4s})} + \frac{W_{ij}}{r_{ij}^6}$$

$$V_{ijk}^3 = B_{jik} e^{(\frac{\gamma}{r_{ij}-r_0} + \frac{\gamma}{r_{ik}-r_0})} \frac{(\cos\theta_{jik} - \cos\bar{\theta}_{jik})^2}{1 + C(\cos\theta_{jik} - \cos\bar{\theta}_{jik})^2}.$$

The two-body terms represent steric repulsion, softened Coulomb forces, charge-dipole, and van der Waals interactions. The three-body terms represent bond bending and stretching. The potential is validated by comparing with experimental measurements [7,8] for various physical properties. These include elastic moduli, phonon dispersion [9], and structural correlations in the crystalline system as well as short-range and medium-range correlations in the amorphous system [6]. The calculated energy of the (110) surface is in reasonable agreement with experiments [10], and the energies of the unreconstructed (111) and (100) surfaces (average of the gallium and arsenic terminated surfaces) are of the same order of magnitude as in *ab initio* calculations [11].

We have also investigated zinc blende to rocksalt structural transformation in bulk Ga-As under pressure. The simulations reveal a reversible transformation from the fourfold coordinated zinc blende structure to a sixfold coordinated rocksalt structure at a pressure of 22 GPa [9]. The calculated variations in the nearest-neighbor distance during the phase transformation agree well with experiment [12] and total-energy calculations [13].

In the simulations reported here, Ga-As nanocrystals are embedded in a hydrostatic pressure medium consisting of a Lennard-Jones (LJ) liquid (with  $\varepsilon = 0.0862$  eV,  $\sigma = 1.30$  Å) [14]. This is analogous to the soft-sphere liquid used in simulations of structural transformation of a silicon cluster [15]. The parameters of the LJ potential are chosen such that the system remains in the liquid state [16] over a wide range of pressures at the operating temperature. The interaction between Ga or As atoms and the surrounding liquid is chosen to be the repulsive part of the LJ interaction. The strength of the repulsive interaction is adjusted to prevent LJ atoms from entering the Ga-As nanocrystal (with  $\tilde{\varepsilon} = 0.101$  eV,  $\tilde{\sigma} = 2.2$  Å).

One of the initial configurations of the nanocrystal is a sphere cut out of bulk Ga-As in zinc blende structure. This spherical nanoparticle is placed in a cavity inside a face-centered-cubic lattice of LJ atoms. To investigate the sensitivity of the structural transformation to the initial shape and surface structure, we also consider a faceted nanocrystal obtained by Wulff construction using average energies of the Ga and As terminated {100} and {111} surfaces and the energy of the {110} surface [17]. The density of the LJ lattice is chosen so that the LJ liquid at the simulation temperature is at the liquid and gas-liquid phase boundary [16]. The temperature of this initial configuration of the LJ system with an embedded Ga-As nanocrystal is increased by scaling atomic velocities and the system is run for  $\sim 10\,000$  time steps (MD time step = 2.18 fs) in the microcanonical ensemble. After melting the LJ lattice, we switch over to the isothermal-isobaric ensemble [18]. The system is thermalized at a pressure of 2.5 GPa for  $\sim 10\,000$  time steps. Subsequently, the pressure is raised in steps of 2.5 GPa over 5000 time steps and the system is thermalized for 10 000–65 000 time steps at each new value of the applied pressure [19]. This procedure is continued until the embedded nanocrystal undergoes a structural transformation.

For spherical nanocrystals of diameter 60 Å, a second simulation schedule is also adopted [14]. The structural transformation is monitored continuously as the pressure is increased linearly at the rate of 2.5 GPa over 10 000 time steps (MD time step = 2 fs). Simulations of spherical nanocrystals involve a single nanoparticle in an LJ liquid, whereas faceted nanocrystals are studied singly or as an ensemble of eight (initially identical) nanocrystals randomly placed in the LJ liquid. The eight nanoparticle simulation contains approximately 40 000 Ga and As atoms and three million LJ atoms.

One set of quantities we calculate to monitor the progress of the structural transformation are the bond angle distributions (average of the Ga-As-Ga and the As-Ga-As bond angles). The distributions are spatially resolved into spherical shells of 5 Å in thickness. The evolution of these distributions indicates that the transformation in both spherical and faceted nanocrystals

nucleates at the surface and proceeds inwards with increasing pressure [14,20]. When the distribution corresponding to the innermost shell develops a peak around  $90^\circ$ , it is taken as an indication of the complete transformation from the zinc blende to the rocksalt phase. With an increase in the nanocrystal size (Fig. 1), the transformation pressure approaches the bulk value [9] from below (the critical pressure is 10.0, 15.0, 17.5, and 22.5 GPa for nanocrystals of diameters 20, 30, 44, and 60 Å, respectively).

Calculations on nanocrystals in vacuum and at  $T = 0$  K suggest that the nanocrystal-liquid interface enthalpy is the driving force for the observed trend in the transformation pressure with increasing diameter of the nanoparticles. The zero-temperature calculations involve spherical nanocrystals of diameters 20, 30, 44, and 60 Å in the zinc blende structure and corresponding transformed structures. In each case, 512 spherical nanocrystals are cut out of an ideal lattice with the centers of the spheres uniformly distributed in the zinc blende primitive unit cell. Six transformed structures are constructed corresponding to each possible transformation mechanism in the bulk. The transformation pressure is determined from the equality of the enthalpy of the original and transformed structures as their lattice constants are varied. Figure 2 shows the variation of the transformation pressure (averaged over  $6 \times 512 = 3072$  cases) with the nanocrystal diameter. The trend in these zero-temperature calculations is similar to that observed for nanocrystals in the LJ liquid, i.e., the transformation pressure approaches the bulk value from below.

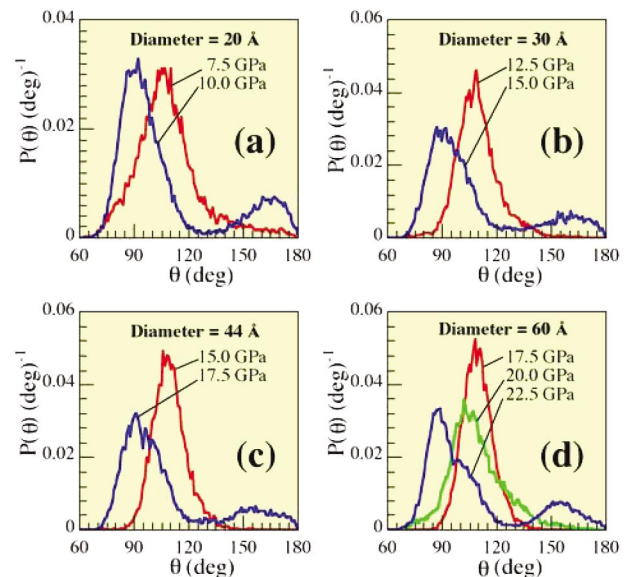


FIG. 1 (color). Averaged Ga-As-Ga and As-Ga-As bond angle distributions corresponding to the interior regions (radius 5 Å) of spherical nanocrystals of diameter (a) 20, (b) 30, (c) 44, and (d) 60 Å. The transformation pressure, identified by the peak around  $90^\circ$ , increases with the nanocrystal size and approaches the bulk value for nanocrystals of diameter 60 Å.

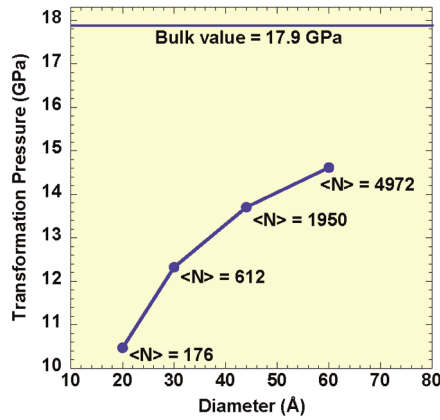


FIG. 2 (color). Variation of the transformation pressure with diameter for nanocrystals in vacuum at zero temperature.  $\langle N \rangle$  is the number of nanocrystal atoms averaged over 512 cases with different centers uniformly distributed in the primitive unit cell of the zinc blende lattice. The zero-temperature bulk value is also shown.

This suggests that the nanocrystal-liquid interface enthalpy is the thermodynamic driving force that determines the dependence of the transformation pressure on the nanocrystal size.

The structure of the transformed nanocrystal is characterized by *local* deformation (strain relative to the zinc blende lattice) of the nanocrystal upon transformation. A one-to-one correspondence between bond formation during transformation and deformation is used to uniquely identify regions of distinct strains [14]. This correspondence is based on the transformation mechanism observed in simulations of bulk silicon carbide [21] and Ga-As [9]. Figure 3 shows spherical nanocrystals of different sizes after transformation. Strains are color-coded onto atoms based on new bonds that atoms form during the transformation. We find multiple colors indicating nonuniform deformation in all the cases. Smaller nanocrystals of diameters 20 Å and 30 Å [Figs. 3(a) and 3(b)] show a single domain structure without any domain boundaries. Nanocrystals of diameter 44 Å [Fig. 3(c)] manifest a multiple domain structure [Fig. 3(d)] with three orientationally distinct strain domains (colored red, cyan, and magenta) and a grain boundary between adjacent domains (cyan and magenta). The largest nanocrystal (diameter 60 Å) shows three strain domains [Fig. 3(e)] (yellow, cyan, and magenta) with two of the adjacent strain domains (cyan and yellow) having nearly the same orientation and no grain boundary between them [14,20]. This illustrates that different strains (relative to the initial zinc blende lattice) do not necessarily lead to different domain orientations.

The pressure at which faceted nanocrystals completely transform is close to that for spherical nanocrystals of equal numbers of atoms. Faceted and spherical nanocrystals consisting of  $\sim 2000$  atoms complete transformations at 17.5 GPa. A faceted nanocrystal with  $\sim 5000$  atoms

transforms completely at 20 GPa, which is slightly less than that for a spherical nanocrystal of diameter 60 Å. The transformed faceted nanocrystal shows significant structural variations from a spherical nanocrystal. In some cases, where these nanocrystals transform into a domain with a single orientation [Figs. 4(a) and 4(c)], they undergo nonuniform deformation and end up with more than one type of strain domain. This single grain structure is observed in three out of nine cases in nanocrystals with  $\sim 2000$  atoms and four out of nine nanocrystals with  $\sim 5000$  atoms. In the remaining cases [Figs. 4(b) and 4(d)], the structure of transformed nanocrystals is similar to that of spherical nanocrystals with domains of distinct orientation separated by grain boundaries. Figure 4(d) also shows that even when the strains relative to the zinc blende lattice are equal, the final orientation of domains can be different due to the relative rotation that domains undergo to maintain connectivity within the nanocrystal (see the magenta domain with different orientations on adjacent sides of the cyan-

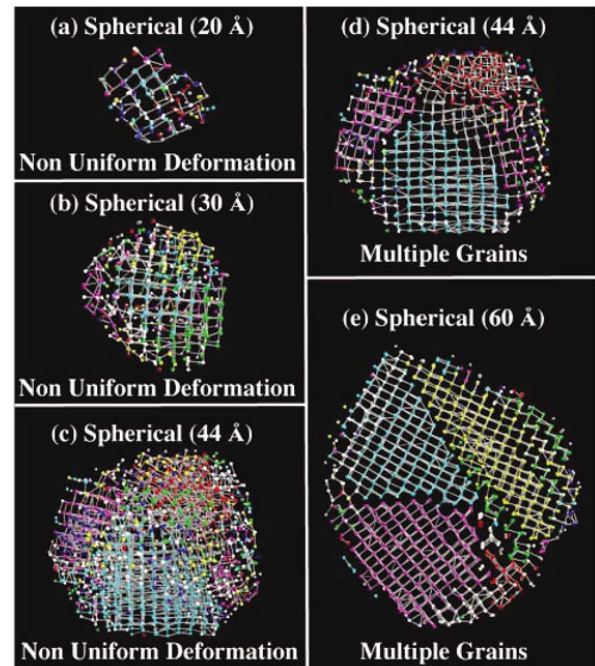


FIG. 3 (color). Strain domains after the structural transformation in spherical nanocrystals. (a), (b), and (c) show nanocrystals of diameter 20, 30, and 44 Å, respectively. (d) and (e) are 12 Å wide cross sections through the middle of the nanocrystals of diameters 44 Å and 60 Å, respectively, that show multiple grains and grain boundaries. Domains are color-coded according to their strains relative to the initial zinc blende lattice. There are six domains identified here by bright colors. Grey color represents regions that have not undergone a significant transformation and where atoms have not formed any new bonds. In the white region, bonds between atoms are different from those formed during the structural transformation in bulk Ga-As. In each strained domain, nearest-neighbor atoms (within a cutoff distance of 3.2 Å) are shown with bonds between them.

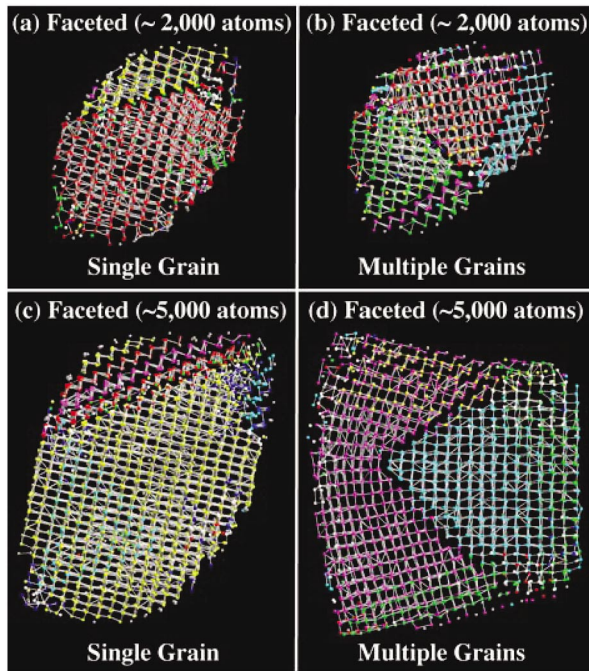


FIG. 4 (color). Strain domains and grains after the structural transformation in faceted nanocrystals with  $\sim 2000$  [(a), (b)] and  $\sim 5000$  [(c), (d)] atoms. (a) and (c) show full nanocrystals. (b) and (d) show  $12 \text{ \AA}$  wide cross section of other nanocrystals. Color-coding scheme is the same as in Fig. 3.

colored domain). In order to remain connected, the region between these domains has a strain over and above that for the structural transformation in the bulk system. This again shows that the domain orientation and strain relative to the zinc blende lattice are not equivalent.

In conclusion, MD simulations of the zinc blende to rocksalt structural transformation in nanocrystals of different sizes and shapes show that with increasing nanocrystal size, the transformation pressure approaches the bulk value from below. Grain boundaries are observed in transformed nanocrystals of sizes equal to or larger than  $44 \text{ \AA}$ . The structure of these nanocrystals shows that the orientation of a transformed region and its strain relative to the zinc blende lattice are inequivalent. Domains of different strains may have the same orientation and domains of distinct orientations may have the same strain relative to the zinc blende lattice. This is important in experimental interpretation, e.g., x-ray line shapes, of the possible mechanisms of structural transformation of nanocrystals.

This work was supported by ARL, AFOSR-USC-DURINT, DOE, NSF, and the Louisiana Board of Regents Health Excellence Fund. The authors thank Hideaki Kikuchi and Fuyuki Shimojo for many useful discussions.

- [1] F.F. Abraham and J.Q. Broughton, Phys. Rev. Lett. **56**, 734 (1986).
- [2] A.N. Goldstein, C.M. Echer, and A.P. Alivisatos, Science **256**, 1425 (1992).
- [3] S.H. Tolbert and A.P. Alivisatos, J. Chem. Phys. **102**, 4642 (1995); S.H. Tolbert, A.B. Herhold, L.E. Brus, and A.P. Alivisatos, Phys. Rev. Lett. **76**, 4384 (1996).
- [4] J.Z. Jiang, J.S. Olsen, L. Gerward, and S. Mörup, Europhys. Lett. **44**, 620 (1998).
- [5] S.B. Qadri, J. Yang, B.R. Ratna, and E.F. Skelton, Appl. Phys. Lett. **69**, 2205 (1996).
- [6] I. Ebbsjö *et al.*, J. Appl. Phys. **87**, 7708 (2000); F.B. Neal, Ph.D. thesis, Louisiana State University, 2004; The three-body softening parameter,  $C = 20$ .
- [7] D. Strauch and B. Dorner, J. Phys. Condens. Matter **2**, 1457 (1990).
- [8] D. Udron *et al.*, J. Non-Cryst. Solids **137-138**, 131 (1991).
- [9] J.P. Rino *et al.*, Phys. Rev. B **65**, 195206 (2002).
- [10] C. Messmer and J.C. Bilello, J. Appl. Phys. **52**, 4623 (1981); R.W. Margevicius and P. Gumbsh, Philos. Mag. A **78**, 567 (1998); G. Michot, A. George, A. Chabli-Brenac, and E. Molva, Scr. Metall. **22**, 1043 (1988).
- [11] J. Wang, M. Needels, and J.D. Jannopoulos, *Surface Science and Related Topics: Festschrift for Xide Xie* (World Scientific, Singapore, 1991), pp. 314–325. (As terminated surfaces,  $(2 \times 2)$  reconstructed (111) surface and the  $2 \times 4$  reconstructed (001) surface, have energies of the same order of magnitude as calculated here for the unreconstructed surfaces).
- [12] J.M. Besson *et al.*, Phys. Rev. B **44**, 4214 (1991).
- [13] S. Froyen and M.L. Cohen, Phys. Rev. B **28**, 3258 (1983).
- [14] S. Kodiyalam, R.K. Kalia, H. Kikuchi, A. Nakano, F. Shimojo, and P. Vashishta, Phys. Rev. Lett. **86**, 55 (2001).
- [15] R. Martonak, C. Molteni, and M. Parrinello, Phys. Rev. Lett. **84**, 682 (2000).
- [16] J.K. Johnson, J.A. Zollweg, and K.E. Gubbins, Mol. Phys. **78**, 591 (1993).
- [17] The Wulff construction reduces surface energy as compared to a spherical nanocrystal. For a nanocrystal with  $\sim 2000$  atoms the average energy per atom decreases by  $0.041 \text{ eV}$ .
- [18] G.J. Martyna, M.E. Tuckerman, D.J. Tobias, and M.L. Klein, Mol. Phys. **87**, 1117 (1996).
- [19] A more rapid schedule is adopted for the spherical nanocrystal of diameter  $60 \text{ \AA}$  in which pressure is increased in steps of  $2.5\text{--}5 \text{ GPa}$  at a rate of  $2.5 \text{ GPa}$  per 500 time steps and thermalization at each pressure is carried out for 5000 steps.
- [20] A. Nakano, T.J. Campbell, R.K. Kalia, S. Kodiyalam, S. Ogata, F. Shimojo, P. Vashishta, and P. Walsh, *Large-Scale Molecular Dynamics Simulations of Materials on Parallel Computers, Advanced Computing and Analysis Techniques in Physics Research: VII International Workshop*, edited by P.C. Bhat and M. Kasemann (American Institute of Physics, Melville, New York, 2001), p. 57.
- [21] F. Shimojo *et al.*, Phys. Rev. Lett., **84**, 3338 (2000).